A Port-Hamiltonian Control Framework to Render a Power Electronic System Passive

Qing-Chang Zhong, *Fellow, IEEE,* and Márcio Stefanello, *Member, IEEE*

***Abstract*—In this note, a control framework is proposed to render a power electronic system passive by adopting the port-Hamiltonian (pH) systems theory. The system has a power electronic converter, either grid-tied or islanded. The control framework consists of a lossless interconnection block and three control channels. It makes the power converter behave as a virtual synchronous machine (VSM). The three channels are designed to, respectively, generate the frequency and the flux of the VSM and a third quantity that is necessary for forming the lossless interconnection. It is proven that the closed-loop system is passive without the need of assuming constant frequency, constant voltage, and/or constant loads. It is sufficient to only assume that the load can be described as a passive pH model. Hence, the proposed control framework is very generic.**

***Index Terms*—Power electronic converter, virtual synchronous machine (VSM), port-Hamiltonian (pH) systems, passivity, distributed generation.**

I. Introduction

The integration of distributed energy resources, such as renewable energy, storage systems and electrical vehicles, into the electrical power system has become a topic of intensive research [1], [2], [3]. Power electronic converters are often used as the interfacing device [2] and the control of power electronic converters is critical to maintain stable and reliable operation of power systems.

Power converters in grid-tied applications are usually current-controlled. That is, there is a primary layer that synthesizes reference currents for power tracking or sharing. However, this may cause detrimental impact [4] on the stability of power systems because the existing power systems are based on synchronous machines that behave as voltage sources. Hence, there is a trend to adopt voltage-controlled power converters. Following this line, some approaches, such as the droop control [5], the virtual synchronous machine (VSM) [6], [7], [8], [9]; controllers based on the Kuramoto oscillator [10] and dispatchable virtual oscillators [11], [12], have been proposed. Note that the droop control principle plays an important role in all of these approaches.

A challenging problem to be solved in this field is how to guarantee the stability of a power electronic converter, either grid-tied or islanded. A more challenging problem is the stability of a system with multiple converters operated together [13]. Although local stability can be established with small-signal analysis and linearization [14], [15], [16], [17], nonlinearities, such as the calculation of the real power and the reactive power and the coupling effect between frequency and voltage dynamics, make it necessary to adopt nonlinear control techniques. The port-Hamiltonian (pH) systems theory [18], [19], [20], [21], [22], [23] has emerged as a very promising tool to address this problem. Works like [24] and [25] have explored the stability and control of microgrids using pH models. In [26], the analogy between a power electronic converter and a synchronous machine has been established with pH models. Furthermore, the conventional power systems with synchronous generators can be modeled and analyzed with pH models; see e.g. [27]. However, most of the works assume that the voltage, the frequency, and/or the loads are constant. Practically, this is not true and makes it even more challenging to study the stability of this kind of systems.

Because of the significant challenges in directly studying the stability of a power electronic system, either with a single converter or with multiple converters, it is worthwhile studying the passivity of the system as an intermediate step and then studying the stability of the system by bridging the gap between stability and passivity.

In this paper, a generic control framework based on the pH systems theory is proposed to render a power electronic converter passive with the only assumption of loads being passive. The converter can be operated in the grid-tied mode or in the islanded mode. Moreover, the proposed control framework makes the converter behave like a VSM. It consists of a lossless interconnection block and three control channels: a *torque-frequency* channel to generate the frequency, a *quorte-flux* channel to generate the flux, and a third channel introduced to form a lossless interconnection. The new word *quorte,* as coined in [28], represents the quantity that is dual to the torque. The three control channels are designed to render the closed-loop system passive for any loads that are passive. Note that the assumption on the loads being passive is not conservative because most nonlinear loads, including ones with active switching devices, can be modeled as passive pH systems [29], [30].

It is well known that the lossless interconnection of a passive control block and a passive control plant is passive; see e.g. [20], [21], [22], [23]. The novelty of this paper lies in identifying the right pairs of signals, constructing a suitable lossless interconnection, and constructing a passive control block for a power electronic system, without the conventional assumptions of constant voltage, constant frequency and/or constant loads, while incorporating the fundamental principles

Q.-C. Zhong is with the Department of Electrical and Computer Engineering, Illinois Institute of Technology, Chicago, IL 60616, USA, and Syndem LLC, USA. Email: zhongqc@ieee.org.

M. Stefanello is with the Fundação Universidade Federal do Pampa at Alegrete, RS, 97546-550, BR. Email: marciostefanello@unipampa.edu.br.

This work was partially supported by NSF, USA, under award #1810105 and CAPES, BR, under grant No. 99999.006061/2015-00.

of synchronous machines into the control framework.

The rest of this paper is organized as follows. In Section II, some preliminaries are given. In Section III, the mathematical model of the system under consideration, together with the problem formulation, are presented. The control framework is presented in Section IV and the main result about the passivity of the closed-loop system is presented in Section V. Some simulation results are presented in Section VI and conclusions are made in Section VII.

II. Preliminaries

For a dynamic system, the concept of passivity involves in a non-negative function of the state vector x, called the storage function $H_s(x)$. A dynamic system is passive if the energy absorbed by the system over any period of time $[0, t]$ is greater than or equal to the increase in the energy stored in the system over the same period, that is, if

$$\int_0^t u^T(\tau)\, y(\tau)\, d\tau \geq H_s(x(t)) - H_s(x(0)). \tag{1}$$

Moreover, it is lossless if both sides of (1) are equal or $\frac{dH_s}{dt}(x(t)) = u^T y$.

Passivity is a compositional property and can be studied with different frameworks; see e.g., [31], [32]. The port-Hamiltonian (pH) systems theory [18] offers a systematic mathematical framework for structural modeling, analysis and control of complex networked multi-physics systems with lumped and/or distributed parameters, which interact with the environment through ports. The usual input-state-output form of a pH system [18], [20], [33], [34] is

$$\begin{aligned} \dot{x} &= [J(x) - R(x)] \frac{\partial H(x)}{\partial x} + G(x)\, u \\ y &= G^T(x) \frac{\partial H(x)}{\partial x}, \end{aligned} \tag{2}$$

where $J(x) = -J(x)^T$ is skew-symmetric, $R(x) = R(x)^T$ is symmetric, $u, y \in \mathbb{R}^m$ are the input and output pair of the system, $x = [x_1, \ldots, x_n]^T \in \mathbb{R}^n$ is the state of the system, and $H(x) : \mathbb{R}^n \to \mathbb{R}$ is a smooth function called Hamiltonian of the system. The input and output pair (u, y) forms a power port of the pH system (2) and the product $u^T y$ has the unit of power. Furthermore, if $R(x) \geq 0$ and $H(x)$ is positive semidefinite, then the system (2) is passive with $H(x)$ being a storage function of the system.

III. System Description and Problem Formulation

A. System Description

The control plant under consideration is a three-phase DC/AC power electronic converter connected to the grid. As illustrated in Fig. 1, the converter is represented with an ideal voltage source $e = \begin{bmatrix} e_a & e_b & e_c \end{bmatrix}^T$. This is because a power electronic converter is often operated at a switching frequency much higher than the fundamental frequency and, from the viewpoint of control, the switching effect of the power semiconductor devices can be neglected [2], according to the well-established averaging theory; see e.g. [35].

The converter may be operated in the grid-tied mode or in the islanded mode with the grid breaker closed or open.

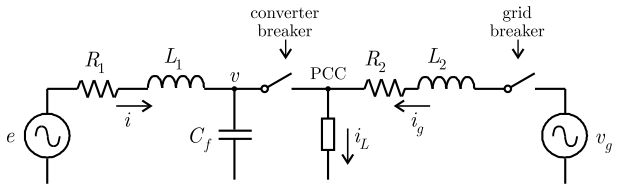

Figure 1: A DC/AC power converter connected to the grid with the converter represented by the voltage source e.

The converter-side L_1 and R_1 model the filter inductor and the capacitor C_f models the filter capacitor. The supply-side elements L_2 and R_2 model the line impedance. Assume that the per-phase load can be represented by the following generalized dissipative pH model [29]:

$$\begin{aligned} M_{Lw}\dot{q}_w &= (J_{Lw} - R_{Lw})\, q_w + G_{Lw} v_w \\ i_{Lw} &= G_{Lw}^T q_w, \end{aligned} \tag{3}$$

where $w = a, b, c$ stands for the three electrical phases with $J_{Lw} = -J_{Lw}^T$, $R_{Lw} = R_{Lw}^T \geq 0$ and $M_{Lw} = M_{Lw}^T$ nonsingular. The converter breaker and the grid breaker are assumed to be closed. By defining the state of the load as $q = \begin{bmatrix} q_a^T & q_b^T & q_c^T \end{bmatrix}^T \in \mathbb{R}^{3m}$, the current drawn by the load as $i_L = \begin{bmatrix} i_{La} & i_{Lb} & i_{Lc} \end{bmatrix}^T$ and the voltage of the load as $v = \begin{bmatrix} v_a & v_b & v_c \end{bmatrix}^T$, the load can be modeled as

$$\begin{aligned} M_L\dot{q} &= (J_L - R_L)\, q + G_L v \\ i_L &= G_L^T q \end{aligned} \tag{4}$$

with $J_L = -J_L^T$, $R_L = R_L^T \geq 0$ and $M_L = M_L^T$ nonsingular, all with appropriate dimensions.

Denote the converter current as $i = \begin{bmatrix} i_a & i_b & i_c \end{bmatrix}^T$, the grid supply current as $i_g = \begin{bmatrix} i_{ga} & i_{gb} & i_{gc} \end{bmatrix}^T$, and the grid supply voltage as $v_g = \begin{bmatrix} v_{ga} & v_{gb} & v_{gc} \end{bmatrix}^T$. Then the system shown in Fig. 1 can be modeled as

$$\begin{aligned} L_1 \frac{di}{dt} &= -R_1 i - v + e, \\ C_f \frac{dv}{dt} &= i - G_L^T q + i_g, \\ L_2 \frac{di_g}{dt} &= -v - R_2 i_g + v_g, \\ M_L \frac{dq}{dt} &= (J_L - R_L)\, q + G_L v. \end{aligned} \tag{5}$$

By defining the state of the plant as

$$x_P = \begin{bmatrix} L_1 i^T & C_f v^T & L_2 i_g^T & (M_L q)^T \end{bmatrix}^T$$

and selecting the Hamiltonian function of the plant as

$$H_P = \frac{1}{2} L_1 i^T i + \frac{1}{2} C_f v^T v + \frac{1}{2} L_2 i_g^T i_g + \frac{1}{2} q^T M_L q, \tag{6}$$

the system (5) can be rewritten as the following pH model

$$\Sigma_P : \begin{cases} \dot{x}_P = (J_P - R_P) \dfrac{\partial H_P}{\partial x_P} + G_P e + G_g v_g \\ i = G_P^T \dfrac{\partial H_P}{\partial x_p} \\ i_g = G_g^T \dfrac{\partial H_P}{\partial x_P} \end{cases} \tag{7}$$

with $\frac{\partial H_P}{\partial x_P} = \begin{bmatrix} i^T & v^T & i_g^T & q^T \end{bmatrix}^T$, $G_P = \begin{bmatrix} I & 0 & 0 & 0 \end{bmatrix}^T$, $G_g = \begin{bmatrix} 0 & 0 & I & 0 \end{bmatrix}^T$,

$$J_P = \begin{bmatrix} 0 & -I & 0 & 0 \\ I & 0 & I & -G_L^T \\ 0 & -I & 0 & 0 \\ 0 & G_L & 0 & J_L \end{bmatrix} \text{ and } R_P = \begin{bmatrix} R_1 I & 0 & 0 & 0 \\ 0 & 0 & 0 & 0 \\ 0 & 0 & R_2 I & 0 \\ 0 & 0 & 0 & R_L I \end{bmatrix}$$

where I is the 3×3 identity matrix. Apparently, the pH system (7) is passive with $H_P \geq 0$, $\forall t$, for any passive load as described in (4). This holds true even when the grid breaker is open, in which case $G_g = \begin{bmatrix} 0 & 0 & 0 & 0 \end{bmatrix}^T$.

B. Problem Formulation

The control problem to be solved in this paper is to design a control law and supply it as the input e for the system shown in Fig. 1 so that the closed-loop system is passive.

IV. Control Framework

A. Control Structure and Control Law

Because of the significance of controlling power electronic converters to behave as VSM [1], [36], the proposed control structure, as shown in Fig. 2, follows the principles of VSM. The closed-loop system consists of a control block Σ_C, an interconnection block Σ_I, and the open-loop plant Σ_P. The control law is designed as

$$e = \omega \varphi \psi z, \tag{8}$$

where $z = \begin{bmatrix} \sin\theta & \sin\left(\theta - \frac{2\pi}{3}\right) & \sin\left(\theta + \frac{2\pi}{3}\right) \end{bmatrix}^T$ with θ being the angle of the phase-a voltage e_a, $\omega = \dot{\theta}$ and φ are the frequency and the virtual flux of the VSM, and ψ is a third variable that is critical for the design and analysis of the system. The control block Σ_C consists of three channels: (T, ω), (Γ, φ), and (Υ, ψ). The quantities T and Γ are the torque of the VSM and its dual quantity *quorte* as coined in [28], respectively, and the quantity Υ is critical for the controller design and analysis. Note that this is different from the conventional VSM design, which only involves in two channels. As will be seen later, the third channel (Υ, ψ) plays a crucial role in rendering the closed-loop system passive.

B. Interconnection Block Σ_I

According to the ghost power theory [1], [37], the active power P and the reactive power Q delivered by the converter can be calculated as

$$P = e^T i \quad \text{and} \quad Q = -e_g^T i, \tag{9}$$

where $e_g = \omega \varphi \psi z_g$ is the ghost signal of e with $z_g = \begin{bmatrix} \cos\theta & \cos\left(\theta - \frac{2\pi}{3}\right) & \cos\left(\theta + \frac{2\pi}{3}\right) \end{bmatrix}^T$ being the ghost signal of z. The real power P and the reactive power Q can be alternatively rewritten as

$$P = \omega T \quad \text{and} \quad Q = \varphi \Gamma, \tag{10}$$

with the torque T and the quorte Γ given as

$$T = \varphi \psi z^T i \quad \text{and} \quad \Gamma = -\omega \psi z_g^T i. \tag{11}$$

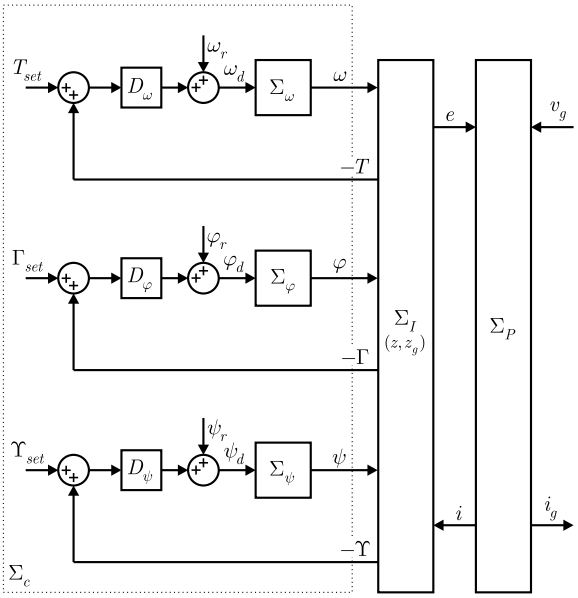

Figure 2: Control framework to render a power electronic system passive

The new quantity Υ is defined as

$$\Upsilon \triangleq -\frac{Q}{\psi} = \omega \varphi z_g^T i. \tag{12}$$

As a result, the interconnection block Σ_I with four ports (e, i), $(-T, \omega)$, $(-\Gamma, \varphi)$, and $(-\Upsilon, \psi)$ can be described as

$$\Sigma_I : \left\{ \begin{bmatrix} e \\ -T \\ -\Gamma \\ -\Upsilon \end{bmatrix} = \begin{bmatrix} 0 & \varphi\psi z & 0 & 0 \\ -\varphi\psi z^T & 0 & -\psi z_g^T i & \varphi z_g^T i \\ 0 & \psi z_g^T i & 0 & 0 \\ 0 & -\varphi z_g^T i & 0 & 0 \end{bmatrix} \begin{bmatrix} i \\ \omega \\ \varphi \\ \psi \end{bmatrix} \right. . \tag{13}$$

It is easy to show that the interconnection block Σ_I is passive because its supply rate is $\varphi\psi\omega z^T i - \varphi\psi\omega z^T i - \varphi\psi\omega z_g^T i + \varphi\psi\omega z_g^T i + \varphi\psi\omega z_g^T i - \varphi\psi\omega z_g^T i = 0$.

C. Design of the Control Block Σ_C

The proposed control block Σ_C, as shown in Fig. 2, consists of three similar channels. The (T, ω) channel generates the frequency ω according to the torque feedback $-T$; the (Γ, φ) channel generates the flux φ according to the quorte feedback $-\Gamma$; and the (Υ, ψ) channel generates ψ according to the feedback $-\Upsilon$. There are many different ways to design these channels. In this paper, these channels are designed according to the droop control principle [1], [38], [39] to satisfy the steady-state performance governed by

$$\omega = \omega_r + D_\omega \left(T_{set} - T\right),$$

$$\varphi = \varphi_r + D_\varphi \left(\Gamma_{set} - \Gamma\right),$$

$$\psi = \psi_r + D_\psi \left(\Upsilon_{set} - \Upsilon\right),$$

where $D_\cdot > 0$ with $\cdot = \omega, \varphi, \psi$ are the droop coefficients, T_{set}, Γ_{set} and Υ_{set} are the set-points for T, Γ and Υ, and ω_r, φ_r and ψ_r are the reference values for ω, φ and ψ that can be

set to their nominal values ω_n, φ_n and ψ_n, respectively. The following low-pass filters

$$\Sigma_{\cdot} = \frac{1}{\tau_{\cdot} s + 1}, \tag{14}$$

with $\tau_{\cdot} > 0$ being the time constants, are adopted to provide the necessary inertia for the frequency channel and to decouple the frequency channel from the φ and ψ channels. Then, the differential equations of the three-channel controllers are

$$\begin{aligned}
\dot{\omega} &= -\frac{1}{\tau_\omega}\omega - \frac{D_\omega}{\tau_\omega}T + \frac{1}{\tau_\omega}\omega_r + \frac{D_\omega}{\tau_\omega}T_{set}, \\
\dot{\varphi} &= -\frac{1}{\tau_\varphi}\varphi - \frac{D_\varphi}{\tau_\varphi}\Gamma + \frac{1}{\tau_\varphi}\varphi_r + \frac{D_\varphi}{\tau_\varphi}\Gamma_{set}, \\
\dot{\psi} &= -\frac{1}{\tau_\psi}\psi - \frac{D_\psi}{\tau_\psi}\Upsilon + \frac{1}{\tau_\psi}\psi_r + \frac{D_\psi}{\tau_\psi}\Upsilon_{set}.
\end{aligned} \tag{15}$$

The set-points T_{set} and Γ_{set} can be chosen as

$$T_{set} = P_{set}/\omega_n \quad \text{and} \quad \Gamma_{set} = Q_{set}/\varphi_n,$$

where φ_n is the nominal value of φ and P_{set} and Q_{set} are the set-points of the real power P and the reactive power Q. Note that the ports $(-\Upsilon,\, \psi)$ and $(-\Gamma,\, \varphi)$ are designed to satisfy $Q = \varphi\Gamma = -\psi\Upsilon$. Hence, it is reasonable to choose $\Upsilon_{set} = -\Gamma_{set}$. Considering the generated voltage in (8) and letting $\psi_n = \varphi_n$, the nominal values φ_n and ψ_n can be obtained as

$$\varphi_n = \psi_n = \sqrt{\sqrt{2}V_n/\omega_n},$$

where V_n is the nominal RMS phase voltage.

V. Main Result

Theorem 1. *The closed-loop system shown in Fig. 2 with the electrical plant (7), the three-channel controllers (15), and the interconnection block (13) is passive for the passive load (4).*

Proof: The three-channel controllers (15) can be rewritten as

$$\begin{cases} \dot{\omega} = -R_\omega \dfrac{\partial H_\omega}{\partial \omega} + G_\omega \left(-T + T_{set} + \frac{1}{D_\omega}\omega_r \right), \\ \omega = G_\omega \dfrac{\partial H_\omega}{\partial \omega} \end{cases} \tag{16}$$

$$\begin{cases} \dot{\varphi} = -R_\varphi \dfrac{\partial H_\varphi}{\partial \varphi} + G_\varphi \left(-\Gamma + \Gamma_{set} + \frac{1}{D_\varphi}\varphi_r \right), \\ \varphi = G_\varphi \dfrac{\partial H_\varphi}{\partial \varphi} \end{cases} \tag{17}$$

$$\begin{cases} \dot{\psi} = -R_\psi \dfrac{\partial H_\psi}{\partial \psi} + G_\psi \left(-\Upsilon + \Upsilon_{set} + \frac{1}{D_\psi}\psi_r \right), \\ \psi = G_\psi \dfrac{\partial H_\psi}{\partial \psi} \end{cases} \tag{18}$$

with $R_{\cdot} = \frac{D_{\cdot}}{\tau_{\cdot}^2}$, $G_{\cdot} = \frac{D_{\cdot}}{\tau_{\cdot}}$ and $H_{\cdot} = \frac{1}{2}\frac{\tau_{\cdot}}{D_{\cdot}}(\cdot)^2$ for $\cdot = \omega,\, \varphi,\, \psi$.

Define $H = H_P + H_\omega + H_\varphi + H_\psi$ and select the state of the closed-loop system as $x = \begin{bmatrix} x_P & \omega & \varphi & \psi \end{bmatrix}^T$. Then H is a Hamiltonian of the closed-loop system with $H \geq 0$. Moreover, after combining (7), (13), (16), (17), and (18), the closed-loop system can be described as

$$\Sigma : \begin{cases} \begin{bmatrix} \dot{x}_P \\ \dot{\omega} \\ \dot{\varphi} \\ \dot{\psi} \end{bmatrix} = \begin{bmatrix} J_P - R_P & G_P G_\omega \varphi\psi z & 0 & 0 \\ -G_\omega \varphi\psi z^T G_P^T & -R_\omega & -G_\varphi G_\omega \psi z_g^T G_P^T \dfrac{\partial H_P}{\partial x_p} & G_\varphi G_\omega G_\psi z_g^T G_P^T \dfrac{\partial H_P}{\partial x_p}\dfrac{\partial H_\varphi}{\partial \varphi} \\ 0 & G_\varphi G_\omega \psi z_g^T G_P^T \dfrac{\partial H_P}{\partial x_p} & -R_\varphi & 0 \\ 0 & -G_\varphi G_\omega G_\psi z_g^T G_P^T \dfrac{\partial H_P}{\partial x_p}\dfrac{\partial H_\varphi}{\partial \varphi} & 0 & -R_\psi \end{bmatrix} \begin{bmatrix} \dfrac{\partial H_P}{\partial x_P} \\ \dfrac{\partial H_\omega}{\partial \omega} \\ \dfrac{\partial H_\varphi}{\partial \varphi} \\ \dfrac{\partial H_\psi}{\partial \psi} \end{bmatrix} \\ \qquad\qquad + \begin{bmatrix} G_g & 0 & 0 & 0 \\ 0 & G_\omega & 0 & 0 \\ 0 & 0 & G_\varphi & 0 \\ 0 & 0 & 0 & G_\psi \end{bmatrix} \begin{bmatrix} v_g \\ T_{set} + \frac{1}{D_\omega}\omega_r \\ \Gamma_{set} + \frac{1}{D_\varphi}\varphi_r \\ \Upsilon_{set} + \frac{1}{D_\psi}\psi_r \end{bmatrix} \\ \begin{bmatrix} i_g \\ \omega \\ \varphi \\ \psi \end{bmatrix} = \begin{bmatrix} G_g & 0 & 0 & 0 \\ 0 & G_\omega & 0 & 0 \\ 0 & 0 & G_\varphi & 0 \\ 0 & 0 & 0 & G_\psi \end{bmatrix} \begin{bmatrix} \dfrac{\partial H_P}{\partial x_P} \\ \dfrac{\partial H_\omega}{\partial \omega} \\ \dfrac{\partial H_\varphi}{\partial \varphi} \\ \dfrac{\partial H_\psi}{\partial \psi} \end{bmatrix} \end{cases} \tag{19}$$

The system (19) is in the pH form of (2) with Hamiltonian $H \geq 0$ and $R(x) = \mathrm{diag}(R_P,\, R_\omega,\, R_\varphi,\, R_\psi) = R^T(x) \geq 0$. Hence, it is passive with respect to the inputs $\left(v_g, \quad T_{set} + \frac{1}{D_\omega}\omega_r, \quad \Gamma_{set} + \frac{1}{D_\varphi}\varphi_r, \quad \Upsilon_{set} + \frac{1}{D_\psi}\psi_r \right)$ and the outputs $\left(i_g, \quad \omega, \quad \varphi, \quad \psi \right)$.

This holds true even when it is operated in the islanded mode as well, in which case the grid breaker is open and $G_g = \begin{bmatrix} 0 & 0 & 0 & 0 \end{bmatrix}^T$. This concludes the proof. ∎

Table I: Electrical and control system parameters.

Parameter	Value	Parameter	Value
L_1, L_2	2.5 mH, 0.5 mH	D_ω	0.14
$R_1 = R_2$	0 Ω	D_φ	4.12×10^{-6}
C_f	15 μF	D_ψ	4.12×10^{-7}
RL load	6.26 Ω, 6.64 mH	τ_ω	0.0001
V_n, f_n	110 V, 60 Hz	τ_φ	0.001
$\varphi_n = \psi_n$	$\sqrt{\frac{\sqrt{2}V_n}{\omega_n}} = 0.64$	τ_ψ	0.01

VI. Simulation Example

Simulations were carried out for a 10 kVA three-phase system depicted in Fig. 1. The electrical and control parameters are summarized in Table I. Note that the self-synchronization strategy proposed in [8] is adopted to facilitate the simulation. As a result, the controller can work in the synchronization mode to synchronize the converter with the grid, in the set mode to send the set real power and reactive power to the grid, and in the droop mode to regulate the system frequency and voltage. It can also work in the islanded mode with the droop functions on.

The results are shown in Fig. 3 with the details explained below.

1) Operation in the Synchronization Mode.

At $t = 0$ sec, the power set-points are set to 0 and the converter starts synchronization with the grid voltage. The grid frequency is set at 59.8Hz and the initial phase angle is set at 45°. The values of T, Γ and Υ are synthesized using the virtual current $i_v = \frac{5}{0.005s+1}(e - v)$. This causes large spikes in P and Q but it does not matter because they are virtual.

At $t = 2$ sec, the converter is connected to the grid, very smoothly without noticeable transients in the currents.

2) Operation in the Set Mode

At $t = 4$ sec, the real power set-point P_{set} is changed to 4 kW. The active power P is regulated to P_{set} (and, thus, T to T_{set}). Accordingly, there are some transients in the frequency.

At $t = 6$ sec, the reactive power set-point Q_{set} is changed to 1 kVar. The reactive power Q is regulated to Q_{set} quickly (and, thus, Γ to Γ_{set} and Υ to Υ_{set}).

At $t = 8$ sec, a grid voltage sag of 10% is applied. There are short large spikes on P and Q mainly due to numerical calculation because the currents and the frequency behave well, except some very short transients. The real power and the reactive power sent to the grid in the steady state remain nearly unchanged. The output voltage dropped accordingly.

3) Operation in the Droop Mode

At $t = 10$ sec, the droop functions of ω, φ and ψ are enabled by setting $\omega_r = \omega_n$, $\varphi_r = \varphi_n$ and $\psi_r = \psi_n$. The real power sent to the grid increases because the grid frequency 59.8 Hz is 0.2 Hz below the nominal frequency.

At $t = 12$ sec, the grid frequency is restored from 59.8 Hz to the nominal value of 60 Hz. The converter frequency changes accordingly without visible impact on φ and ψ, nor on Γ or Υ. As a result, no big changes are observed on the rms voltage or on the reactive power.

4) Islanded Operation with Droop Functions on

At $t = 14$ sec, the converter is disconnected from the grid to operate without a local load. The real power and reactive power drop to close to 0. Since φ reaches a value of 0.6502, the corresponding theoretical rms value of e is $\frac{\omega\varphi\psi}{\sqrt{2}} \to \frac{\omega_n\varphi\psi_n}{\sqrt{2}} = 111.34$ V, very close to the measured rms voltage of 111.6 V. Note that P_{set} is still 4kW so the frequency is about 60.25Hz.

At $t = 16$ sec, a three-phase 5 kW, 2 kVar inductive load is connected. The frequency drops to slightly below 60 Hz.

At $t = 18$ sec, the set-points P_{set} and Q_{set} are changed to zero. The frequency and the voltage drop accordingly while P and Q remain nearly unchanged because the load remains unchanged.

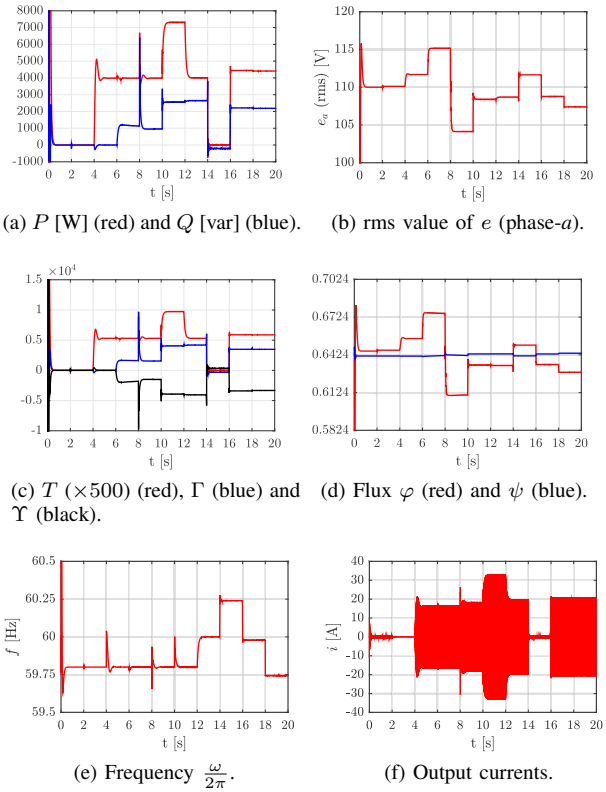

(a) P [W] (red) and Q [var] (blue). (b) rms value of e (phase-a).

(c) T (×500) (red), Γ (blue) and Υ (black). (d) Flux φ (red) and ψ (blue).

(e) Frequency $\frac{\omega}{2\pi}$. (f) Output currents.

Figure 3: Simulation results.

VII. Conclusion

In this paper, a control framework has been proposed to guarantee the passivity of a power electronic converter, either grid-tied or islanded, using the port-Hamiltonian systems theory. The major challenge lies in identifying the right pairs of signals, constructing a suitable lossless interconnection block, and constructing a passive control block with the right number of control channels. The proposed control structure consists of a lossless interconnection block and three control channels. The passivity of the closed-loop system is rigorously proven. No assumptions are made about the line impedance, the voltage or the frequency. The only assumption is that the load can be described by a passive port-Hamiltonian model. Note that this assumption is not too conservative because most nonlinear loads, including ones with active switching devices, can be modeled as pH systems [29], [30]. The results in this paper can also be applied to render loads that have a front-end power electronic converter passive if needed. Hence, the proposed control framework is very generic.

The next step is to study the asymptotic stability of the system via bridging the gap between passivity and stability. For this, the dissipation obstacle [23] needs to be investigated. While it is not going to be straightforward, it is very promising from the simulations results given in this paper. Another interesting topic for future research is to find out whether there exists a two-channel structure to render the system passive. It is also worth studying whether the assumption on loads being passive is a necessary condition as well.

REFERENCES

[1] Q.-C. Zhong, *Power Electronics-Enabled Autonomous Power Systems: Next Generation Smart Grids*. Wiley-IEEE Press, 2020.

[2] Q.-C. Zhong and T. Hornik, *Control of Power Inverters in Renewable Energy and Smart Grid Integration*. Wiley-IEEE Press, 2013.

[3] J. Carrasco, L. Franquelo, J. Bialasiewicz, E. Galvan, R. Portillo-Guisado, M. Prats, J. Leon, and N. Moreno-Alfonso, "Power-electronic systems for the grid integration of renewable energy sources: A survey," *IEEE Trans. Ind. Electron.*, vol. 53, no. 4, pp. 1002–1016, Jun. 2006.

[4] B. Wen, D. Boroyevich, R. Burgos, P. Mattavelli, and Z. Shen, "Small-signal stability analysis of three-phase ac systems in the presence of constant power loads based on measured d-q frame impedances," *IEEE Trans. Power Electron.*, vol. 30, no. 10, pp. 5952–5963, Oct 2015.

[5] Q.-C. Zhong, "Robust droop controller for accurate proportional load sharing among inverters operated in parallel," *IEEE Trans. Ind. Electron.*, vol. 60, no. 4, pp. 1281–1290, Apr. 2013.

[6] H.-P. Beck and R. Hesse, "Virtual synchronous machine," in *Proc. of the 9th International Conference on Electrical Power Quality and Utilisation (EPQU)*, 2007, pp. 1–6.

[7] Q.-C. Zhong and G. Weiss, "Static synchronous generators for distributed generation and renewable energy," in *Proc. of IEEE PES Power Systems Conference & Exhibition (PSCE)*, Mar. 2009, pp. 1–6.

[8] Q.-C. Zhong, P.-L. Nguyen, Z. Ma, and W. Sheng, "Self-synchronised synchronverters: Inverters without a dedicated synchronisation unit," *IEEE Trans. Power Electron.*, vol. 29, no. 2, pp. 617–630, Feb. 2014.

[9] Q.-C. Zhong, "Power electronics-enabled autonomous power systems: Architecture and technical routes," *IEEE Trans. Ind. Electron.*, vol. 64, no. 7, pp. 5907–5918, Jul. 2017.

[10] J. W. Simpson-Porco, F. Dörfler, and F. Bullo, "Synchronization and power sharing for droop-controlled inverters in islanded microgrids," *Automatica*, vol. 49, no. 9, pp. 2603–2611, 2013.

[11] G.-S. Seo, M. Colombino, I. Subotic, B. Johnson, D. Groß, and F. Dörfler, "Dispatchable virtual oscillator control for decentralized inverter-dominated power systems: Analysis and experiments," in *2019 IEEE Applied Power Electronics Conference and Exposition (APEC)*. IEEE, 2019, pp. 561–566.

[12] M. Colombino, D. Groß, J.-S. Brouillon, and F. Dörfler, "Global phase and magnitude synchronization of coupled oscillators with application to the control of grid-forming power inverters," *IEEE Transactions on Automatic Control*, vol. 64, no. 11, pp. 4496–4511, 2019.

[13] S. Liu, P. X. Liu, and X. Wang, "Stability analysis of grid-interfacing inverter control in distribution systems with multiple photovoltaic-based distributed generators," *IEEE Trans. Ind. Electron.*, vol. 63, no. 12, pp. 7339–7348, Dec 2016.

[14] H. Wu, X. Ruan, D. Yang, X. Chen, W. Zhao, Z. Lv, and Q.-C. Zhong, "Small-signal modeling and parameters design for virtual synchronous generators," *IEEE Trans. Ind. Electron.*, vol. 63, no. 7, pp. 4292–4303, July 2016.

[15] N. Pogaku, M. Prodanović, and T. C. Green, "Modeling, analysis and testing of autonomous operation of an inverter-based microgrid," *IEEE Trans. Power Electron.*, vol. 22, no. 2, pp. 613–625, 2007.

[16] X. Guo, Z. Lu, B. Wang, X. Sun, L. Wang, and J. M. Guerrero, "Dynamic phasors-based modeling and stability analysis of droop-controlled inverters for microgrid applications," *IEEE Trans. Smart Grid*, vol. 5, no. 6, pp. 2980–2987, 2014.

[17] A. D. Paquette and D. M. Divan, "Virtual impedance current limiting for inverters in microgrids with synchronous generators," *IEEE Trans. Ind. Appl.*, vol. 51, no. 2, pp. 1630–1638, 2015.

[18] A. van der Schaft and D. Jeltsema, "Port-Hamiltonian systems theory: An introductory overview," *Foundations and Trends in Systems and Control*, vol. 1, no. 2-3, pp. 173–378, 2014. [Online]. Available: http://dx.doi.org/10.1561/2600000002

[19] B. Maschke and A. Van Der Schaft, "Port controlled Hamiltonian systems: modeling origins and system theoretic properties," in *IFAC Symp. Nonlinear Control Systems Design*, 1991, pp. 359–365.

[20] R. Ortega, A. van der Schaft, F. Castanos, and A. Astolfi, "Control by interconnection and standard passivity-based control of port-Hamiltonian systems," *IEEE Transactions on Automatic Control*, vol. 53, no. 11, pp. 2527–2542, Dec. 2008.

[21] R. Ortega and J. G. Romero, "Robust integral control of port-Hamiltonian systems: The case of non-passive outputs with unmatched disturbances," *Systems & Control Letters*, vol. 61, no. 1, pp. 11–17, 2012.

[22] S. Fiaz, D. Zonetti, R. Ortega, J. M. A. Scherpen, and A. J. Van der Schaft, "A port-Hamiltonian approach to power network modeling and analysis," *European Journal of Control*, vol. 19, no. 6, pp. 477–485, 2013.

[23] R. Ortega, A. J. van der Schaft, I. Mareels, and B. Maschke, "Putting energy back in control," *IEEE Control Systems*, vol. 21, no. 2, pp. 18–33, 2001.

[24] J. Schiffer, R. Ortega, A. Astolfi, J. Raisch, and T. Sezi, "Conditions for stability of droop-controlled inverter-based microgrids," *Automatica*, vol. 50, no. 10, pp. 2457–2469, 2014.

[25] J. Schiffer, E. Fridman, R. Ortega, and J. Raisch, "Stability of a class of delayed port-hamiltonian systems with application to microgrids with distributed rotational and electronic generation," *Automatica*, vol. 74, pp. 71–79, 2016.

[26] C. Arghir, T. Jouini, and F. Dörfler, "Grid-forming control for power converters based on matching of synchronous machines," *Automatica*, vol. 95, pp. 273–282, 2018.

[27] A. van der Schaft and T. Stegink, "Perspectives in modeling for control of power networks," *Annual Reviews in Control*, vol. 41, pp. 119–132, 2016.

[28] Q.-C. Zhong and M. Stefanello, "Port-Hamiltonian control of power electronic converters to achieve passivity," in *Proc. of the 56th IEEE Conference on Decision and Control*, Dec 2017.

[29] G. C. Konstantopoulos and A. T. Alexandridis, "Generalized nonlinear stabilizing controllers for Hamiltonian-passive systems with switching devices," *IEEE Trans. Control Syst. Technol.*, vol. 21, no. 4, pp. 1479–1488, 2013.

[30] C. Gaviria, E. Fossas, and R. Grino, "Robust controller for a full-bridge rectifier using the IDA approach and GSSA modeling," *IEEE Trans. Circuits Syst. I*, vol. 52, no. 3, pp. 609–616, 2005.

[31] M. Xia, P. J. Antsaklis, V. Gupta, and F. Zhu, "Passivity and dissipativity analysis of a system and its approximation," *IEEE Trans. Autom. Control*, vol. 62, no. 2, pp. 620–635, Feb 2017.

[32] F. Zhu, M. Xia, and P. J. Antsaklis, "On passivity analysis and passivation of event-triggered feedback systems using passivity indices," *IEEE Trans. Autom. Control*, vol. 62, no. 3, pp. 1397–1402, March 2017.

[33] D. Jeltsema and A. Doria-Cerezo, "Port-Hamiltonian formulation of systems with memory," *Proceedings of the IEEE*, vol. 100, no. 6, pp. 1928–1937, June 2012.

[34] B. Maschke, R. Ortega, and A. J. V. D. Schaft, "Energy-based Lyapunov functions for forced Hamiltonian systems with dissipation," *IEEE Transactions on Automatic Control*, vol. 45, no. 8, pp. 1498–1502, Aug. 2000.

[35] B. Lehman and R. M. Bass, "Extensions of averaging theory for power electronic systems," *IEEE Trans. Power Electron.*, vol. 11, no. 4, pp. 542–553, 1996.

[36] Q.-C. Zhong, "Virtual synchronous machines: A unified interface for smart grid integration," *IEEE Power Electronics Magazine*, vol. 3, no. 4, pp. 18–27, Dec 2016.

[37] ——, "The ghost operator and its applications to reveal the physical meaning of reactive power for electrical and mechanical systems and others," *IEEE Access*, vol. 5, pp. 13 038–13 045, 2017.

[38] Q.-C. Zhong and Y. Zeng, "Universal droop control of inverters with different types of output impedance," *IEEE Access*, vol. 4, pp. 702–712, Jan. 2016.

[39] Q.-C. Zhong, W. L. Ming, and Y. Zeng, "Self-synchronized universal droop controller," *IEEE Access*, vol. 4, pp. 7145–7153, Oct. 2016.